Heliyon 10 (2024) e30969

Contents lists available at ScienceDirect

Heliyon

journal homepage: www.cell.com/heliyon

Research article

Atrase A, a P-III class metalloproteinase purified from cobra venom, exhibits potent anticoagulant activity by inhibiting coagulation pathway and activating the fibrinolytic system

Xin-Jie Zhong [a,b,c], Cai-E Wang [c,d], Ya-Nan Li [a,c], Qi-Yun Zhang [a,c], Qian-Yun Sun [a,b,c,*]

[a] State Key Laboratory of Functions and Applications of Medicinal Plants, Guizhou Medical University, Guiyang, 550014, China
[b] School of Pharmaceutical Sciences, Guizhou Medical University, Guiyang, 550025, China
[c] Natural Products Research Center of Guizhou Province, Guiyang, 550014, China
[d] Department of Pharmacy, The First Affiliated Hospital, and College of Clinical Medicine of Henan University of Science and Technology, Luoyang, 471003, China

ARTICLE INFO

Keywords:
Snake venom metalloproteinases
Anticoagulation
Coagulation factor VIII
Tissue-type fibrinogen activator
Cobra venom

ABSTRACT

Snake venoms, comprising a complex array of protein-rich components, an important part of which are snake venom metalloproteinases (SVMPs). These SVMPs, which are predominantly isolated from viperid venoms, are integral to the pathology of snakebites. However, SVMPs derived from elapid venoms have not been extensively explored, and only a handful of SVMPs have been characterized to date. Atrase A, a nonhemorrhagic P-III class metalloproteinase from *Naja atra* venom, exhibits weak proteolytic activity against fibrinogen in vitro but has pronounced anticoagulant effects in vivo. This contrast spurred investigations into its anticoagulant mechanisms. Research findings indicate that atrase A notably extends the activated partial thromboplastin time, diminishes fibrinogen levels, and impedes platelet aggregation. The anticoagulant action of atrase A primarily involves inhibiting coagulation factor VIII and activating the endogenous fibrinolytic system, which in turn lowers fibrinogen levels. Additionally, its effect on platelet aggregation further contributes to its anticoagulant profile. This study unveils a novel anticoagulant mechanism of atrase A, significantly enriching the understanding of the roles of cobra venom metalloproteinases in snake venom. Furthermore, these findings underscore the potential of atrase A as a novel anticoagulant drug, offering insights into the functional evolutions of cobra venom metalloproteinases.

1. Introduction

Snakebites constitute a global public health concern and result in more than one million fatalities annually [1,2]. Snake venom serves as the primary causative agent of snakebites. It comprises a complex mixture of toxins with diverse toxicological manifestations, including neurotoxicity, hematotoxicity, and cytotoxicity [3]. Snake venom consists of a plethora of enzymes and nonenzymatic constituents. The nonenzymatic components primarily include three-finger toxins (3FTxs), C-type lectin-like proteins, and disintegrins, among others [4,5]. Enzymatic constituents include serine proteases, metalloproteinases, phospholipases A_2, and amino acid oxidases

* Corresponding author. Natural Products Research Center of Guizhou Province, 3491 Baijin Avenue, Guiyang, 550014, China.
E-mail address: sunqianyun@gmc.edu.cn (Q.-Y. Sun).

https://doi.org/10.1016/j.heliyon.2024.e30969
Received 30 January 2024; Received in revised form 7 May 2024; Accepted 8 May 2024
Available online 12 May 2024

[6,7]. Notably, snake venom metalloproteinases (SVMPs) represent a significant protein category that is predominantly sourced from viperid venoms, with only a limited presence in elapid venoms [8,9]. Based on the structural composition disparities of SVMPs, they are categorized into three main classes: P–I, which exclusively features a metalloproteinases domain; P-II, which comprises a metalloproteinase domain and a disintegrin domain; and P-III, which includes a cysteine structural domain in addition to the aforementioned two structural domains. P-IIIs can be further subdivided into four subtypes, P-IIIa, P-IIIb, P-IIIc, and P-IIId, owing to their structural intricacies [10–12]. SVMPs primarily target plasma proteins, platelets, and vascular endothelial cells, resulting in systemic or localized hemorrhage, procoagulation, edema, inflammation, and myonecrosis [13–17]. To date, SVMPs have been isolated predominantly from viperid venoms [12], as elapid venom contains a limited amount of metalloproteinase with weak proteolytic activity, leading to the isolation of only a few metalloproteinases from elapid venoms [18]. It has been demonstrated that P-III class metalloproteinases from viperid venoms disrupt the vascular basement membrane, leading to significant hemorrhagic effects [19–23]. In contrast to SVMPs from viperid venoms, metalloproteinases in elapid venoms lack hemorrhagic activity. However, the structural basis underlying these disparities in activity remains to be fully elucidated. Consequently, it is of scientific significance to investigate SVMPs derived from cobra venoms.

Atrase A and atrase B, both P-III class metalloproteinases, were isolated from Naja atra venom [24,25]. Our previous study revealed the weak proteolytic activity of them against fibrinogen in vitro; nevertheless, they displayed notable anticoagulant activity in vivo. Therefore, this paper explores the efficient anticoagulant effect of atrase A and elucidates the underlying anticoagulant mechanism involved.

2. Materials

The lyophilized crude venom of *Naja atra* was obtained from the Natural Products Research Center of Guizhou Province. Protein purification was performed with gels acquired from GE HealthCare Technologies, Inc. Standard human plasma and coagulation factor II, V, VII, VIII, IX, X, XI, and XII deficient plasmas assay kits were obtained from Siemens Healthcare Diagnostics Products GmbH (Marburg, Germany). Additionally, coagulation factors V, IX, X, XI, and XII were obtained from Haematologic Technologies, Inc. (HTI, USA); factor VIII was sourced from Shanghai RAAS Blood Products Co., Ltd. (Shanghai, China); and factor II was obtained from Enzyme Research Laboratories Ltd. (Swansea, UK). Polyvinylidene fluoride (PVDF) was acquired from Sigma–Aldrich. Factor VIII polyclonal antibody (PA5-106877) was obtained from Thermo Fisher Scientific, Inc., and anti-rabbit IgG and HRP-linked antibody (7074S) were obtained from Cell Signaling Technology, Inc. Chemical compounds such as arachidonic acid (AA), adenosine diphosphate (ADP), thrombin (Thr), and aspirin were purchased from Sigma (USA). Collagen (ALEX, USA), thrombin time (TT), prothrombin time (PT), activated partial thromboplastin time (APTT), and fibrinogen (FIB) assay kits were obtained from Shanghai Sun Biotechnology Co., Ltd. (Shanghai, China). Thromboelastography kits were purchased from Beijing Lepu Biopharma Co., Ltd. (Beijing, China). Enzyme-linked immunosorbent assay kits for D-dimer, fibrin degradation products (FDP), tissue plasminogen activator (t-PA), fibrinolytic enzyme complex plasmin-α2-antiplasmin complex (PAP), and plasminogen activator inhibitor-1 (PAI-1) were obtained from Shanghai Westang Biotech Co., Ltd. (Shanghai, China). The chromogenic substrate S-2238 and chromogenic substrate S-2251 were obtained from Shanghai Boatman Biotech Co., Ltd. (Shanghai, China). All the other reagents used were of analytical purity.

Male Sprague Dawley rats weighing 200–250 g were procured from Changsha Tianqin Biotechnology Co., Ltd. The experimental animals were handled in accordance with a protocol approved by the Institutional Animal Care and Use Committee of Guizhou Medical University (No.2304039).

3. Methods

3.1. Purification and preparation of atrase A

Atrase A was purified using methods previously established in our research [24]. Once dissolved, the venom of *Naja atra* was subjected to sequential passage through SP Sephadex C-25, Sephacryl S-200, and HiTrap Heparin HP chromatography columns. The resulting preparation exhibited homogeneity, as confirmed by both reducing and nonreducing sodium dodecyl sulfate-polyacrylamide gel electrophoresis (SDS-PAGE). Subsequently, the purified product was quantified, divided into aliquots, and preserved at −80 °C for future use.

3.2. In vitro anticoagulation assay

For APTT and PT assays, 100 μL of standard human plasma was combined with 20 μL of atrase A at various concentrations. In the TT assay, 200 μL of standard human plasma was blended with 40 μL of atrase A at various concentrations. Moreover, in the fibrinogen concentration assay, 200 μL of standard human plasma was mixed with 40 μL of atrase A at different concentrations. Subsequently, all the mixtures were incubated at 37 °C for 5 or 30 min, after which the clotting time was determined following the instructions of the kit.

3.3. In vivo anticoagulation assay

3.3.1. Sample preparation

The rats were segregated into different groups of six to ten rats each, which received injections of PBS or atrase A at doses of 0.3 mg/kg, 1.5 mg/kg, or 3 mg/kg, respectively. Each dose of atrase A group was divided into different time points groups according to the

sampling time. At 0.3 mg/kg of atrase A, sampling time points groups were 2, 6, 12, and 24 h. At 1.5 mg/kg of atrase A, sampling times points groups were 2, 6, 12, 24, 48, 72, and 96 h. At 3.0 mg/kg of atrase A, sampling times points groups were 2, 6, 12, 24, 48, 120 and 192 h. Blood samples were collected from the abdominal aorta of rats after injection of atrase A and after anesthesia by intraperitoneal injection of sodium pentobarbital (40 mg/kg) half an hour before the different time intervals. Anticoagulant whole blood was prepared using a solution of 0.109 mol/L sodium citrate. Subsequently, the anticoagulant whole blood was subjected to centrifugation at 140×*g* for 10 min to yield platelet-rich plasma (PRP). Subsequent centrifugation at 2000×*g* for 15 min was performed to obtain platelet-poor plasma (PPP). The remaining anticoagulant whole blood was subjected to centrifugation at 2000×*g* for 15 min to isolate the plasma, which was aliquoted and stored at −80 °C until further use.

3.3.2. Coagulation assay

The groups of anticoagulated plasma samples were tested for APTT, PT, TT, and FIB according to the kit instructions.

3.3.3. Platelet aggregation assay

The platelet counts in the PRP were standardized to 3×10^{11} platelets per liter by diluting with PPP. Subsequently, the induced platelet aggregation rates in response to AA (1.5 mM), ADP (0.02 mM), thrombin (3 U/mL), and collagen (10 μg/mL) were assessed using a platelet aggregometer. The platelet aggregation measurements were conducted by adding 270 μL of adjusted PRP, followed by the addition of the respective inducer via an AG400 platelet aggregometer (Beijing Purui Instrument Co., Ltd., Beijing, China).

3.4. Coagulation factor assay

3.4.1. Factor-deficient plasma assay

To screen the effect of undiluted factor-deficient plasma on target proteins, a procedure involving 50 μL of deficient factor plasma mixed with 50 μL of atrase A-treated standard human plasma with a final concentration of 100 μg/mL in a test tube. Subsequently, 100 μL of APTT reagent was added, followed by incubation for 5 min at 37 °C. Afterward, 100 μL of prewarmed $CaCl_2$ at 37 °C was introduced, and the clotting time was recorded. For PT determination, 50 μL of spent factor plasma was combined with 50 μL of incubated plasma in a test tube. Then, 200 μL of prewarmed PT reagent was added at 37 °C, and the clotting time was recorded. PBS served as the control for the samples. Further investigation into the effect of target proteins on coagulation factors was carried out using serial dilutions of factor-deficient plasma. Coagulation times were assessed for a series of plasma dilutions. The activities of the 1:5, 1:10, 1:50, and 1:500 dilutions to be 100 %, 50 %, 10 %, and 1 %, respectively, of the standard values. A double logarithmic curve was constructed, with assay time plotted on the vertical axis and coagulation factor activity on the horizontal axis. The activity of coagulation factors in atrase A-treated plasma (1:5) was then calculated as a percentage of the normal value according to the reference curve. The residual activity of the coagulation factors was expressed as a percentage of the standard value and indicated on the reference curve. The inhibition rate was calculated as follows: 100 % minus the residual activity of coagulation factors, expressed as a percentage of the standard value.

3.4.2. SDS–PAGE and Western blot

Coagulation factors (2 μg) were incubated with various concentrations of atrase A at 37 °C for various durations. Specifically, 0.4 μg of atrase A was employed with factors II and VIII, while 0.67 μg of atrase A was utilized with factor V. Atrase A at a concentration of 1 μg was employed with factors IX, X, XI, and XII. Subsequently, factors V and VIII were assessed using 6 % SDS–PAGE under reducing conditions, with the remaining factors analyzed using 10 % SDS–PAGE.

For Western blot analysis, 2 μg of coagulation factor VIII was incubated with 0.4 μg of atrase A at 37 °C for 6 h. Following denaturation, the samples were resolved using 10 % SDS–PAGE and transferred onto a PVDF membrane. After a 1 h blocking step at room temperature, the membrane was subjected to incubation with factor VIII polyclonal antibody (dilution: 1:1000) at 4 °C overnight. Subsequently, the membrane was washed with TBST, followed by incubation with an anti-rabbit HRP-linked antibody (dilution: 1:1000) at room temperature for 1 h. After further washing with TBST, the membrane was imaged using VisionCapt v16.15 software (Vilber Lourmat, France).

3.4.3. Coagulation correction assay

To investigate the effect of atrase A, 20 μL of atrase A at a final concentration of 100 μg/mL was mixed with 100 μL of standard human plasma and incubated at 37 °C for 30 min. Subsequently, 100 μL of this plasma was combined with varying concentrations of coagulation factors, and APTT was promptly measured.

For in vivo plasma correction, 100 μL of anticoagulated plasma was withdrawn from rats that had received intravenous injections of atrase A at a dose of 0.3 mg/kg via the tail vein for 1 h. Following this, APTT was immediately measured after the addition of the appropriate quantities of coagulation factors [26], with an additional 20 μL of solution.

3.5. Chromogenic assay

The rats were divided into different groups, with six rats in each group, and received injections of PBS or atrase A at doses of 0.03 mg/kg or 0.3 mg/kg, respectively. Following the administration of atrase A, the rats were anesthetized with an intraperitoneal injection of sodium pentobarbital (40 mg/kg) half an hour prior to the collection of blood samples from the abdominal aorta of the rats at different time points. Anticoagulant whole blood was centrifuged at 2000×*g* for 15 min to obtain anticoagulant plasma for the assay.

For the chromogenic substrate assay, 0.01 mg/mL of Protobothrops mucrosquamatus (PMV) served as the positive control, while PBS was used as the negative control. Thrombin and plasmin activities were assessed using the chromogenic substrates S-2251 (4 mM) and S-2238 (4 mM). A total volume of 100 μL was used, the incubation time was 4 h, and measurements were taken at 15 min intervals. The absorbance at 405 nm was quantified using a Synergy HTX multifunctional enzyme instrument (Molecular Devices, LLC, USA). In vitro, atrase A was detected through incubation with coagulation factor II and the chromogenic substrate. The final concentration of atrase A used was 100 μg/mL. In vivo, plasma, PBS, and the chromogenic substrate were mixed thoroughly and assessed at a constant temperature of 37 °C while shielded from light.

3.6. Fibrinolytic activity assay

The rats were segregated into different groups, with six rats in each group, and received intravenous injections through the tail vein of PBS or atrase A at doses of 0.03 mg/kg or 0.3 mg/kg. Blood samples were collected from the abdominal aorta at various time points, and plasma was prepared as previously described. Following the manufacturer's instructions, enzyme-linked immunosorbent assays (ELISAs) for t-PA, PAI-1, PAP, D-dimer, and FDP were conducted using postdosing plasma and blank plasma. Absorbance values were measured using a Synergy HTX multifunctional enzyme instrument.

3.7. Comparison of anticoagulant activity and platelet aggregation activity

The rats were divided different three groups, with six rats in each group, and received intravenous injections through the tail vein of PBS, 0.03 mg/kg, or 0.3 mg/kg of atrase A. Blood samples were collected from the abdominal aorta at various time points, and whole blood, PRP, PPP, and plasma were prepared as previously described. The dose of atrase A was reduced to 0.03 mg/kg to facilitate a comparison between anticoagulant activity and platelet aggregation inhibition activity. Whole blood was subjected to thromboelastography, PRP was utilized for platelet aggregation assays, and anticoagulated plasma was used for the detection of coagulation parameters and ELISA. Anticoagulated whole blood derived from the test samples was analyzed using a CFMSLEPU-8800 Thromboelastograph (Beijing LEPU Biopharmaceutical Co., Ltd., Beijing, China) in accordance with the instructions provided with the thromboelastography kit.

3.8. Antithrombotic assay

Rats were randomly assigned to four groups: the sham group (sham), the model group (model), and the high-dose (3.0 mg/kg) and low-dose (0.3 mg/kg) anticoagulant atrase A groups, each comprising eight to nine rats. The high- and low-dose atrase A groups received a single dose via tail vein injection 1.5 h prior to modeling. The aspirin group was orally administered for three consecutive days, starting three days before surgery and continuing once more before modeling.

Anesthesia was induced in all the rat groups by intraperitoneal injection of 0.6 mol/L pentobarbital (0.3 g/kg) 15 min after drug administration. Following anesthesia, both common carotid arteries were isolated. The right common carotid artery was prepared for blood collection, while the left common carotid artery was isolated to a length of 2 cm. A small piece of plastic film (4 cm × 1.8 cm) was placed beneath it to protect the perivascular tissues. In all groups except the sham-operated group, a small piece of filter paper (1 cm × 1 cm) containing 20 μL of $FeC1_3$ (2.16 mol/L) solution was applied to the left common carotid artery. In the sham-operated group, an equal amount of saline-soaked filter paper was used. After 30 min of modeling, the blood vessels at the site of thrombosis in the left common carotid artery were promptly excised, placed on filter paper to absorb any residual blood, and weighed using an electronic analytical balance.

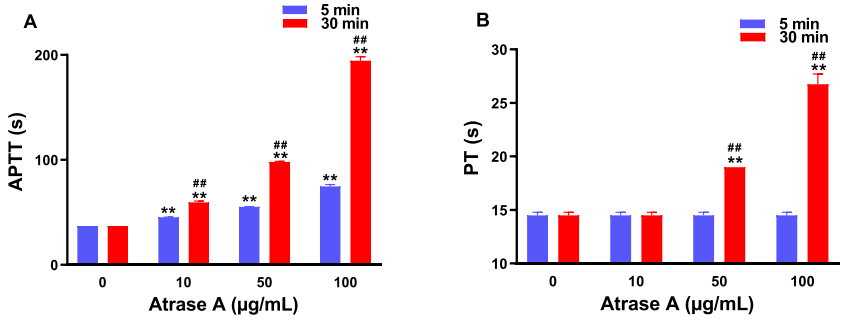

Fig. 1. Effects of atrase A on coagulation in vitro A and B represent the effects of incubating atrase A with human standard plasma for 5 and 30 min at 10, 50 and 100 μg/mL on APTT and PT, respectively. The results are presented as the mean ± SD (n = 4). $^{**}P < 0.01$ *vs* control. $^{\#\#}P < 0.01$, *vs* incubation for 5 min.

3.9. Statistical analysis

All the data are presented as the means ± SDs. The statistical analysis was conducted using SPSS version 27.0.1 software. Comparisons between two groups were performed using an independent samples *t*-test, while comparisons among multiple groups were

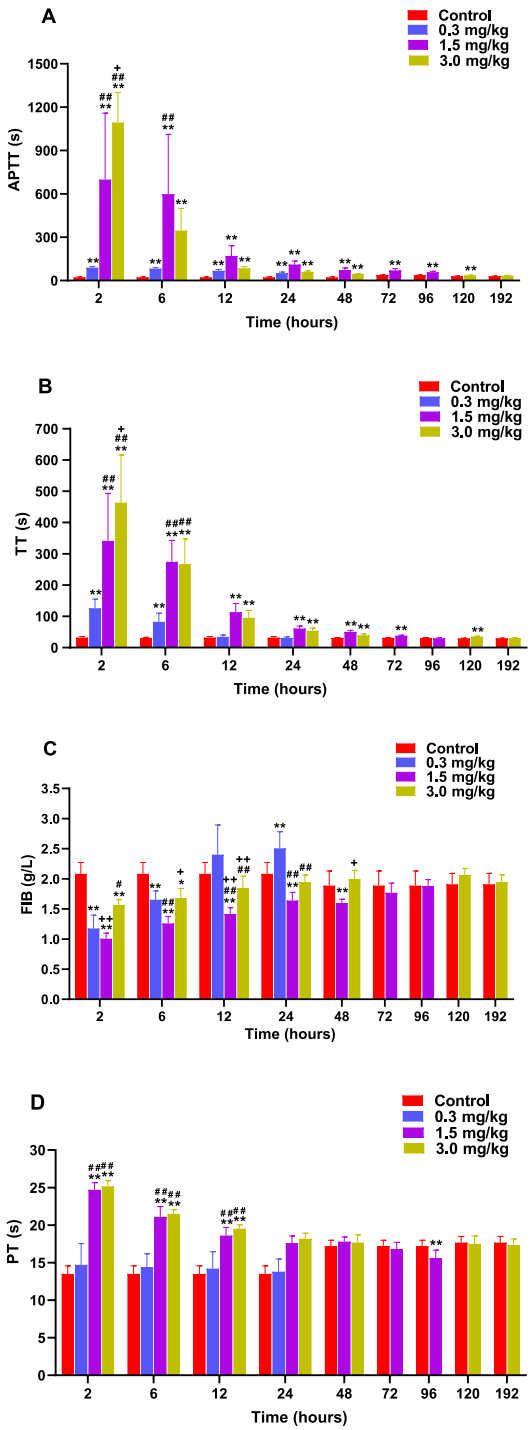

Fig. 2. Effect of atrase A on coagulation in vivo Anticoagulated plasma was obtained at different times after different concentrations of atrase A were injected into rats for the APTT, TT, fibrinogen and PT assays. From A to D represent APTT, TT, fibrinogen, and PT, respectively. The results are presented as the mean ± SD (n = 6–10). $^{*}P < 0.05$, $^{**}P < 0.01$ *vs* control. $^{\#}P < 0.05$, $^{\#\#}P < 0.01$ *vs* 0.3 mg/kg $^{+}P < 0.05$, $^{++}P < 0.01$ *vs* 1.5 mg/kg.

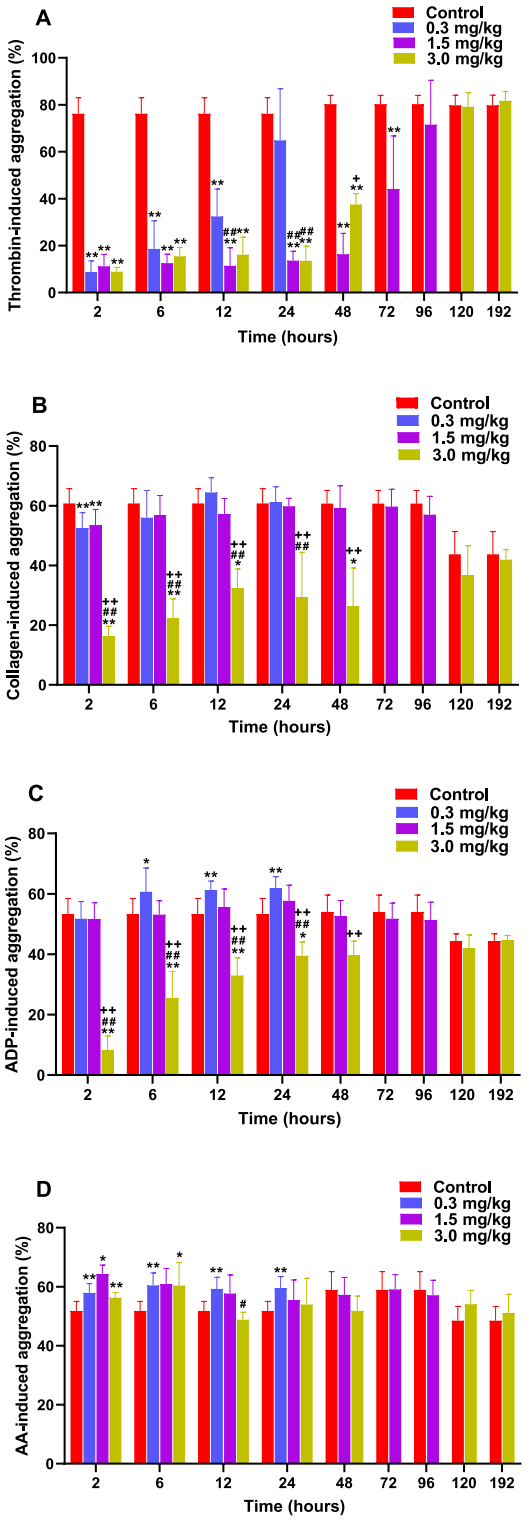

Fig. 3. Effect of atrase A on platelet function in vivo A to D correspond to the effects induced on platelet aggregation in rats at different time intervals following tail vein injections of 0.3 mg/kg, 1.5 mg/kg, and 3 mg/kg of atrase A. PRP platelet counts were adjusted to 3×10^{11} platelets/L using PPP, 270 μL of adjusted PRP was mixed with 5 μL of inducer. Subsequently, the platelet aggregation rates induced by AA (1.5 mM), ADP (0.02 mM), Thr (3 U/mL), and collagen (10 μg/mL) were measured via platelet aggregometry. The results are presented as the mean ± SD (n = 6–10). $^{*}P < 0.05$, $^{**}P < 0.01$ *vs* control. $^{\#}P < 0.05$, $^{\#\#}P < 0.01$ *vs* 0.3 mg/kg $^{+}P < 0.05$, $^{++}P < 0.01$ *vs* 1.5 mg/kg.

carried out using one-way ANOVA. $P < 0.05$ was considered to indicate statistical significance.

4. Results

4.1. In vitro anticoagulant activity

In vitro anticoagulation experiments revealed that incubation with varying doses of atrase A led to a noteworthy prolongation of APTT at 5 min (Fig. 1A). Moreover, this incubation for 30 min at 50 μg/mL and 100 μg/mL also significantly prolonged PT (Fig. 1B). However, it had no discernible effect on TT or fibrinogen levels under identical experimental conditions (Supplementary materials Figs. S1A and B).

4.2. In vivo anticoagulant activity

4.2.1. Coagulation function assay

The experimental results revealed notable prolongation of both APTT and TT (Fig. 2A and B), accompanied by a reduction in fibrinogen levels at all three administered doses (Fig. 2C). Specifically, APTT returned to normal after 192 h with the 3 mg/kg dose. Furthermore, at doses of 1.5 mg/kg and 3 mg/kg, PT was significantly extended (Fig. 2D).

4.2.2. Platelet aggregation

The experimental findings revealed a substantial inhibitory effect on thrombin- and collagen-induced platelet aggregation across all three administered doses (Fig. 3A and B). Notably, thrombin-induced aggregation did not return to normal levels until 96 h after treatment with the 1.5 mg/kg dose (Fig. 3A). Additionally, ADP-induced aggregation was significantly suppressed at the 3 mg/kg dose (Fig. 3C). No inhibitory effect was showing on AA-induced platelet aggregation (Fig. 3D).

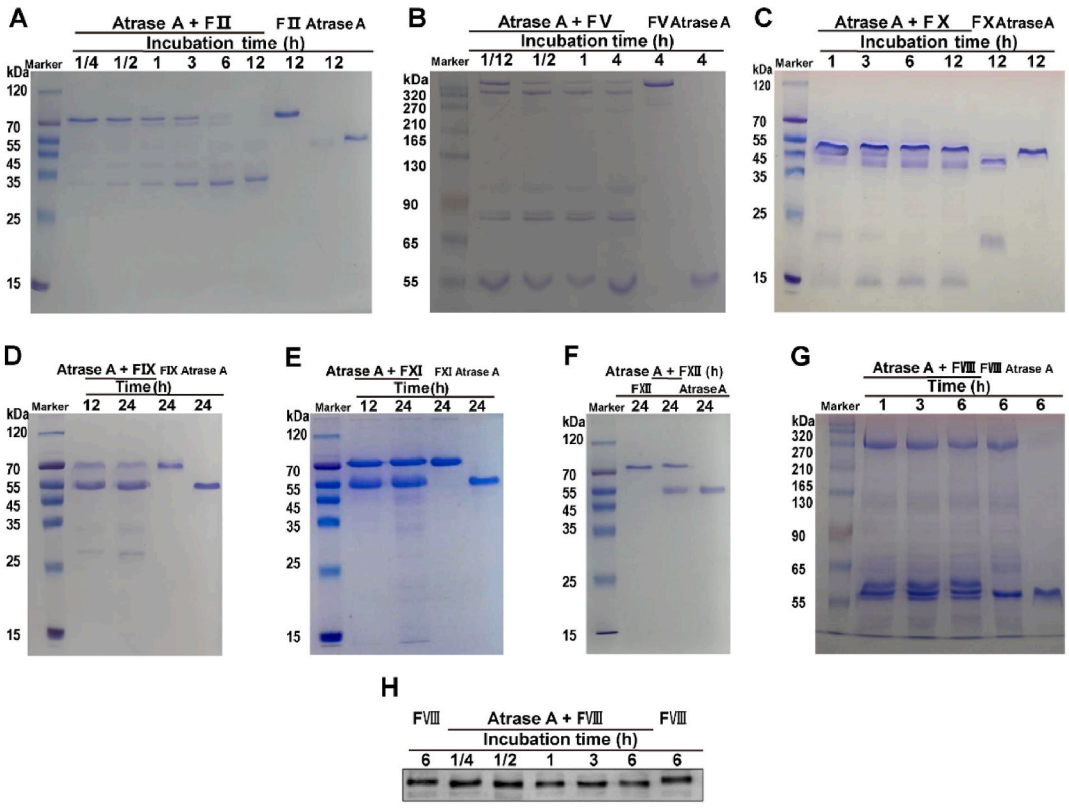

Fig. 4. Assay for incubation mixture of atrase A and coagulation factor A, B, C, D, E, F, and G represent coagulation factors II, V, X, IX, XI, XII, and VIII, respectively, with each coagulation factor at a concentration of 2 μg. The enzyme-to-substrate ratios used were as follows: 1:5, 1:3, 1:2, 1:2, 1:1, 1:2, 1:2, and 1:2. The separating gel concentrations used for (B) and (G) were 5 %, while the remaining concentrations were 10 %. (H) represents the Western blot result of atrase A cleavage with factor VIII at a ratio of 1:5. Original images are visible in the supplementary materials.

4.3. Action on coagulation factors

4.3.1. Factor-deficient plasma assay

To investigate the effect of atrase A on coagulation factors, the targets of atrase A were assessed using undiluted factor-deficient plasma. The results demonstrated that the target proteins exerted varying effects on each coagulation factor (Supplementary materials Figs. S2A–B). Building upon these findings, the influence of target proteins on coagulation factors was further explored through serially diluted factor-deficient plasma. The inhibition rates were as follows: 98.72 % for coagulation factor VIII, 90.71 % for IX, 86.93 % for XI, 85.15 % for II, 83.30 % for V, 76.05 % for XII, 54.64 % for X, and 18.7 % for VII (Supplementary materials Figs. S3A–H).

4.3.2. Enzyme cleavage coagulation factor assay

Effect of atrase A on cleaving coagulation factors was assayed by SDS-PAGE (Fig. 4A–G). Atrase A and coagulation factor cleavage assays revealed that atrase A effectively cleaved coagulation factors II (Fig. 4A), V (Fig. 4B), X (Fig. 4C), and VIII (Fig. 4H). However, after 24 h of incubation, no cleavage products were detected for factors IX, XI, and XII (Fig. 4D–F). Enzymatic cleavage was complete within 12 h for factor II when the enzyme and substrate were present at a 1:5 ratio (Fig. 4A), within 6 h for factor V at a 1:3 ratio (Fig. 4B), and within 6 h for factor X at a 1:2 ratio (Fig. 4C). Western blot analysis performed with factor VIII at a 1:5 ratio demonstrated no generation of new products after a 15-min incubation with atrase A (Fig. 4H).

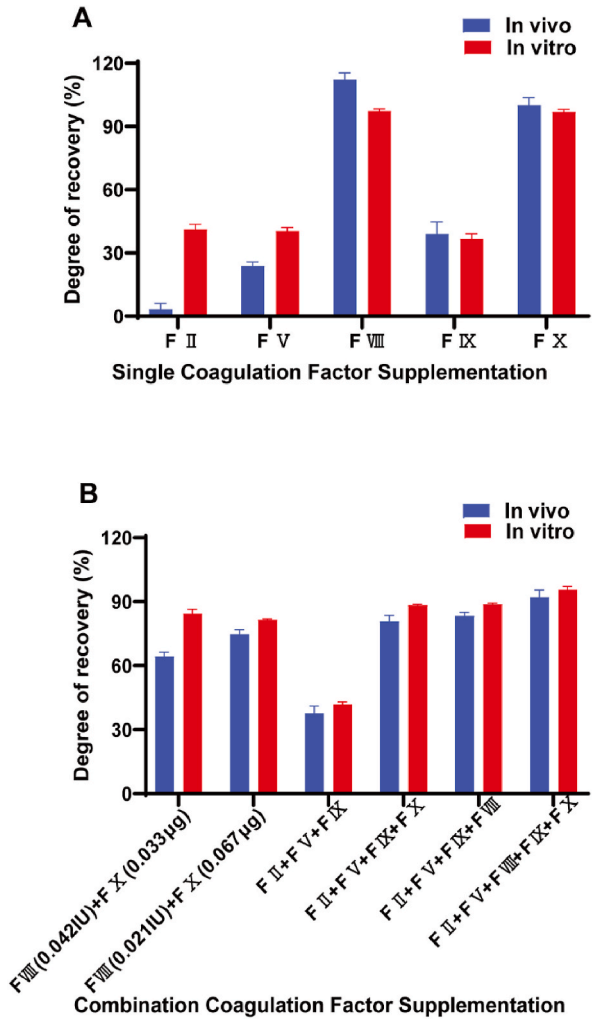

Fig. 5. The degree of recovery of coagulation function by adding coagulation factors In vitro, the final concentration of atrase A was 100 μg/mL, while in vivo, plasma was treated with atrase A at a dose of 0.3 mg/kg through tail vein injection for 1 h. In (A) each coagulation factor was added to the atrase A-treated plasma for APTT detection. Specifically, factor II was added at 10 μg, factor V at 1.32 μg, factor VIII at 3.13 IU, factor IX at 0.51 μg, and factor X at 1 μg. In (B), a combination of coagulation factors was added to the atrase A-treated plasma for APTT, with the following quantities: factor II at 10 μg, factor V at 1.32 μg, factor VIII at 0.042 IU or 0.021 IU, factor IX at 0.51 μg, and factor X at 0.033 μg or 0.067 μg. The summarized results are as follows.

4.3.3. Coagulation factor correction assay

Based on the extent of recovery observed after plasma coagulation factor supplementation following atrase A treatment in vivo, the addition of coagulation factor VIII and coagulation factor X successfully restored APTT to nearly normal levels, achieving recoveries of 97.4 % and 96.9 %, respectively, in the treated plasma in vitro (Fig. 5A). These recoveries were comparable to those observed in vivo (Fig. 5A). Conversely, the addition of coagulation factors II, V, and IX partially restored APTT values, with recoveries in in vitro processed plasma of 41.1 %, 40.5 %, and 36.8 %, respectively (Fig. 5A). In vivo, the corresponding recovery rates were 0.9 %, 23.8 %, and 39.1 %, respectively (Fig. 5A). Furthermore, we investigated the combined addition of coagulation factors to atrase A-treated plasma, revealing that the inclusion of factors II, V, and IX only partially restored coagulation in both in vitro and in vivo processed plasma, resulting in recovery rates of 41.8 % and 37.7 %, respectively (Fig. 5B).

4.4. Effect of atrase A on fibrinogen

4.4.1. Chromogenic assay

These findings indicate that atrase A does not activate thrombin following incubation with coagulation factor II (Supplementary materials Fig. S4). At a dose of 0.03 mg/kg, there was an increase in thrombin activity, which notably elevated enzymatic fibrinolytic activity at 0.5 h and 1 h (Fig. 6A and B). Moreover, the dose of 0.3 mg/kg led to increased thrombin activity at 2 h and a significant increase in plasmin activity at 0.5 h and 1 h (Fig. 6C and D).

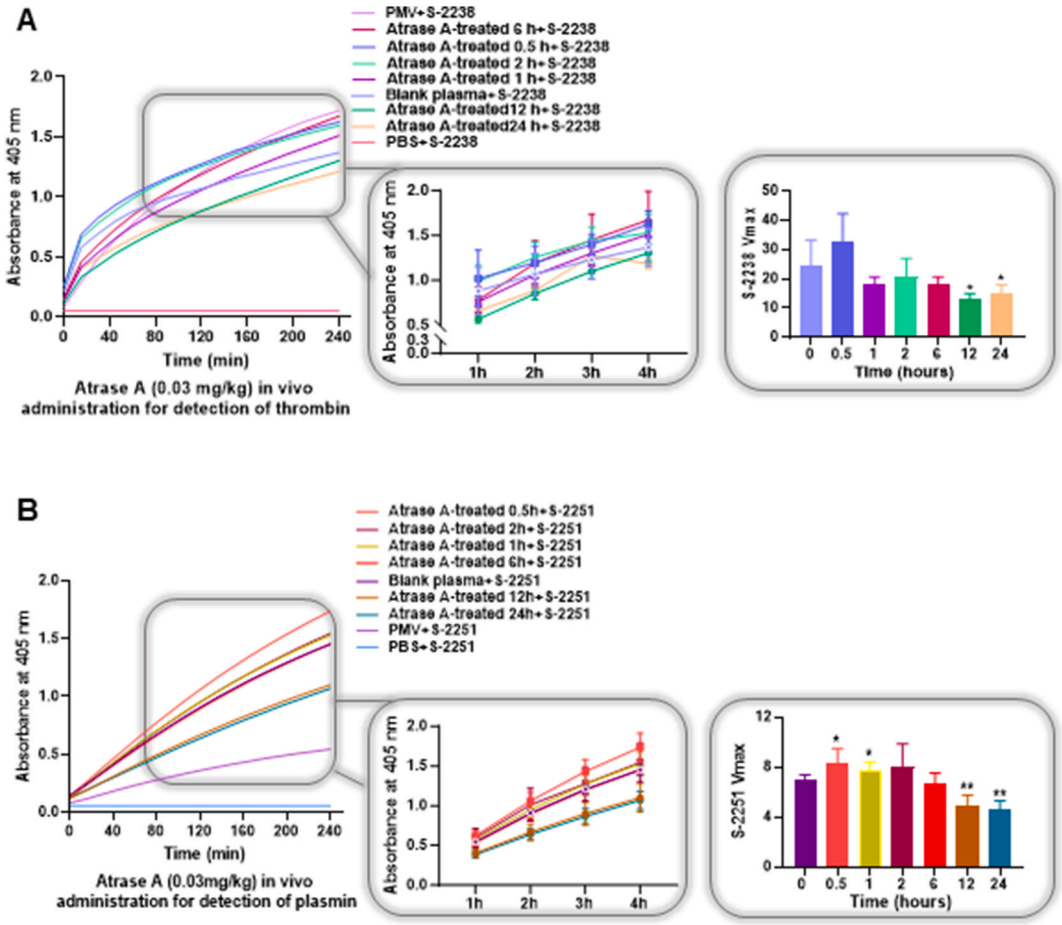

Fig. 6. Effect of atrase A on the activities of fibrinolytic enzymes and thrombin A positive control with 0.01 mg/mL PMV and a negative control with PBS were utilized in the assays. In (A) and (C), 10 μL of plasma, 40 μL of S-2238 chromogenic substrate, and 50 μL of PBS were combined, resulting in a total system volume of 100 μL. For (B) and (D), 20 μL of plasma, 40 μL of S-2251 chromogenic substrate, and 40 μL of PBS were mixed, resulting in a total system volume of 100 μL. After thorough mixing, the samples were incubated at a constant temperature of 37 °C in the dark for 4 h, after which the A405 nm was measured at 15 min intervals. The samples were subjected to atrase A administration at doses of 0.3 mg/kg and 0.03 mg/kg and were analyzed at 0.5 h, 1 h, 2 h, 6 h, 12 h, and 24 h after administration, along with blank plasma. The initial reaction rate was specifically analyzed test data. The results are presented as the mean ± SD (n = 6) $^{*}P < 0.05$, $^{**}P < 0.01$ *vs* control.

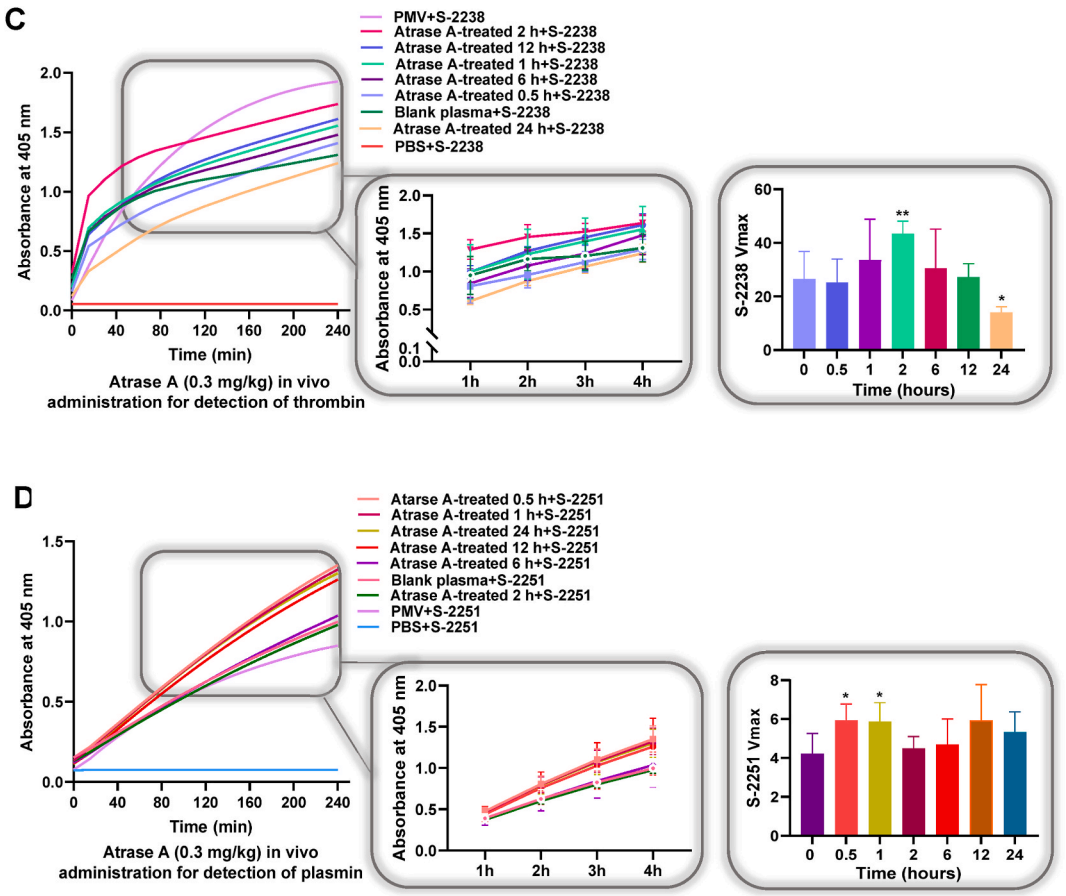

Fig. 6. (*continued*).

4.4.2. Effect of atrase A on the fibrinolytic system

To validate that atrase A induces activation of the fibrinolytic system, we measured FDP and D-dimer levels. The results revealed that at a dose of 0.3 mg/kg, there was a significant increase in FDP content at 1 h and 2 h, accompanied by a substantial increase in D-dimer content at 2 h and 6 h, along with a decrease in fibrinogen (Fig. 7A and B). Notably, these effects were dose dependent.

According to the experimental findings, a low dose (0.3 mg/kg) of the target protein significantly upregulated the t-PA content at 2 h but had no effect on the PAI-1 content (Fig. 8A–C). The medium dose (1.5 mg/kg) induced a moderate increase in both t-PA and PAI-1 levels (Fig. 8D–F). At the high dose (3.0 mg/kg), there was a notable upregulation of t-PA and PAI-1 in rats at 2 h. All three doses significantly elevated PAP levels at 2 h (Fig. 8G–I). Even when the dose was reduced to 0.03 mg/kg, there was a certain degree of upregulation of t-PA and PAI-1, although there was no significant change in PAP content (Fig. 8J-L).

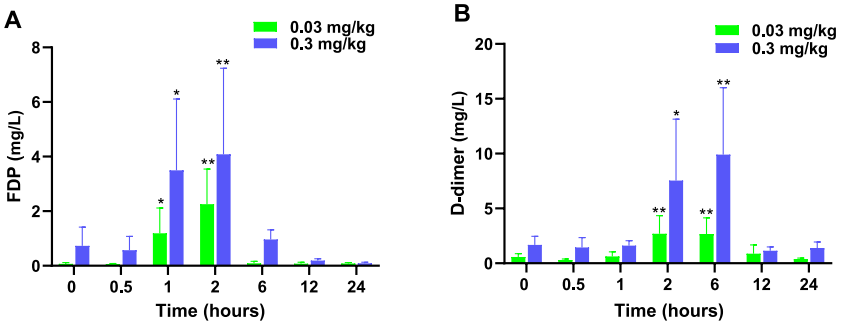

Fig. 7. Assays for FDP and D-dimer levels in plasma after the injection of atrase A A and B represent plasma samples were obtained from rats injected with 0.03 mg/kg or 0.3 mg/kg atrase A via the tail vein after 2 h, 6 h, 12 h, or 24 h to detect the level of FDP and D-dimer. The results are presented as the mean ± SD (n = 6). $^{*}P < 0.05$, $^{**}P < 0.01$ *vs* control.

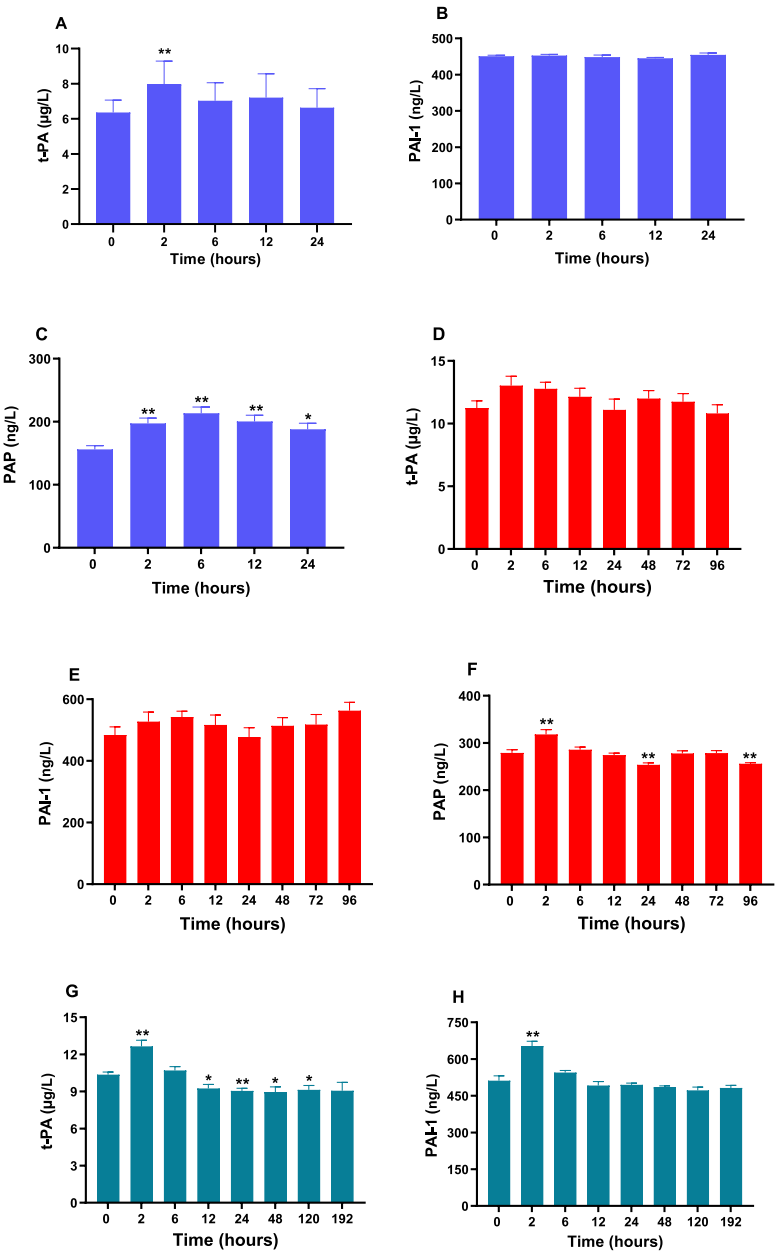

Fig. 8. Assays for t-PA, PAI-1 and PAP in plasma after the injection of atrase A Rats received intravenous tail vein injections of varying doses of atrase A. Plasma samples were collected at different time intervals, and ELISA was conducted to assess the concentrations of t-PA, PAI-1, and PAP. For doses of 0.3 mg/kg (A–C), 1.5 mg/kg (D–F), 3 mg/kg (G–I), and 0.03 mg/kg (J–L), the results are summarized as follows. The results are presented as the mean ± SD (n = 6–10). $^{*}P < 0.05$, $^{**}P < 0.01$ *vs* control.

4.5. *Comparative assays of platelet aggregation and anticoagulation*

Even with a further reduction in the dose of atrase A to 0.03 mg/kg, APTT, TT, and FIB did significantly increase (Fig. 9A–D). Thromboelastography results (Fig. 10A-O), utilizing a more sensitive measurement, demonstrated that the 0.03 mg/kg dose prolonged the R values (Fig. 10K). Importantly, at this lower dose, atrase A did not significantly affect platelet function, but thrombin-induced platelet aggregation activity was enhanced (Fig. 9E).

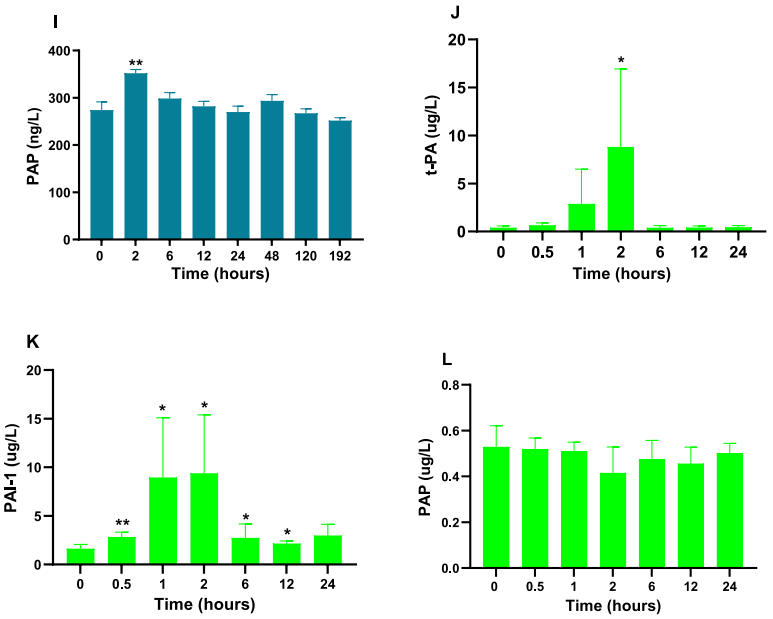

Fig. 8. (*continued*).

4.6. Thromboprophylactic effect

The low-dose atrase A (0.3 mg/kg) effectively prevented thrombosis, and the effect was not significantly different from that of the positive control. Notably, the high-dose group (3.0 mg/kg) exhibited more pronounced and statistically significant inhibition of thrombosis compared to positive control (Fig. 11).

5. Discussion

In our previous studies, atrase A was shown to display weak proteolytic activity against fibrinogen and inhibit platelet aggregation by cleaving GPIb in vitro [27]. However, it exhibited significant anticoagulant activity in vivo, prompting us to investigate this activity and its underlying mechanism. The results indicate that the mechanism of action of atrase A in vivo involves the inhibition of coagulation factors, a reduction in fibrinogen levels, and the inhibition of platelet aggregation.

In vitro incubation of atrase A with plasma significantly prolonged APTT in a dose-dependent manner. It also had a certain effect on PT but no significant effect on TT or fibrinogen levels. In vivo injection of 0.3 mg/kg, 1.5 mg/kg, or 3.0 mg/kg atrase A into rats had significant effects on coagulation and platelet aggregation. There were dose-dependent changes in APTT and TT, with significant effects on PT at doses of 1.5 mg/kg and 3.0 mg/kg. Atrase A most significantly inhibited thrombin-induced platelet aggregation in a dose-dependent manner, consistent with the cleavage of the platelet membrane glycoprotein GPIb mentioned earlier.

Considering the anticoagulant effect of atrase A, we used factor-deficient plasma to assess its inhibitory effect on coagulation factors. The results indicated that atrase A inhibited coagulation factors, with inhibition rates of 98.72 %, 90.71 %, 86.93 %, 85.15 %, and 83.3 % for factors VIII, IX, XI, II, and V, respectively. The inhibition rate for factor VII plasma was 18.7 %. Consequently, we conducted in vitro cleavage experiments using each coagulation factor in combination with atrase A. These experiments showed that atrase A effectively cleaved coagulation factors VIII, II, V, and X, with factor VIII being the most efficiently cleaved. To further verify these findings, we performed recovery experiments by adding coagulation factors to plasma samples treated with atrase A. The results showed that factors II, V, IX, XI, and XII were not the primary targets of atrase A, as their addition only partially restored coagulation function. However, the addition of factor VIII or X completely restored coagulation. According to the results of factor-deficient plasma experiments, the inhibition rates of coagulation factor VIII and X were 98.72 % and 54.64 %, respectively. In enzyme cleavage experiments, factor VIII was completely cleaved within 15 min, while factor X was cleaved within 6 h. In vitro plasma incubation experiments showed that while PT remained unaffected, APTT was significantly prolonged. In vivo experiments prolonged APTT and TT, with an effect on PT observed only after increasing the dose. From these experiments, we can conclude that factor VIII is the most suitable substrate for atrase A, and the prolongation of PT is likely due to the cleavage of factor X. Coagulation factor X occupies a crucial position in the coagulation cascade [28], thus, supplement of factor X also can significantly restore the coagulation function. As for the prolongation of TT, it is related with the decrease of fibrinogen levels. The cleavage of coagulation factor VIII by atrase A results in a product of approximately 5 kD, and it is assumed that this fragment is located in the active region of factor VIII [29]. Further investigations into the enzymatic reaction kinetics of atrase A cleavage of coagulation factor VIII and X are warranted.

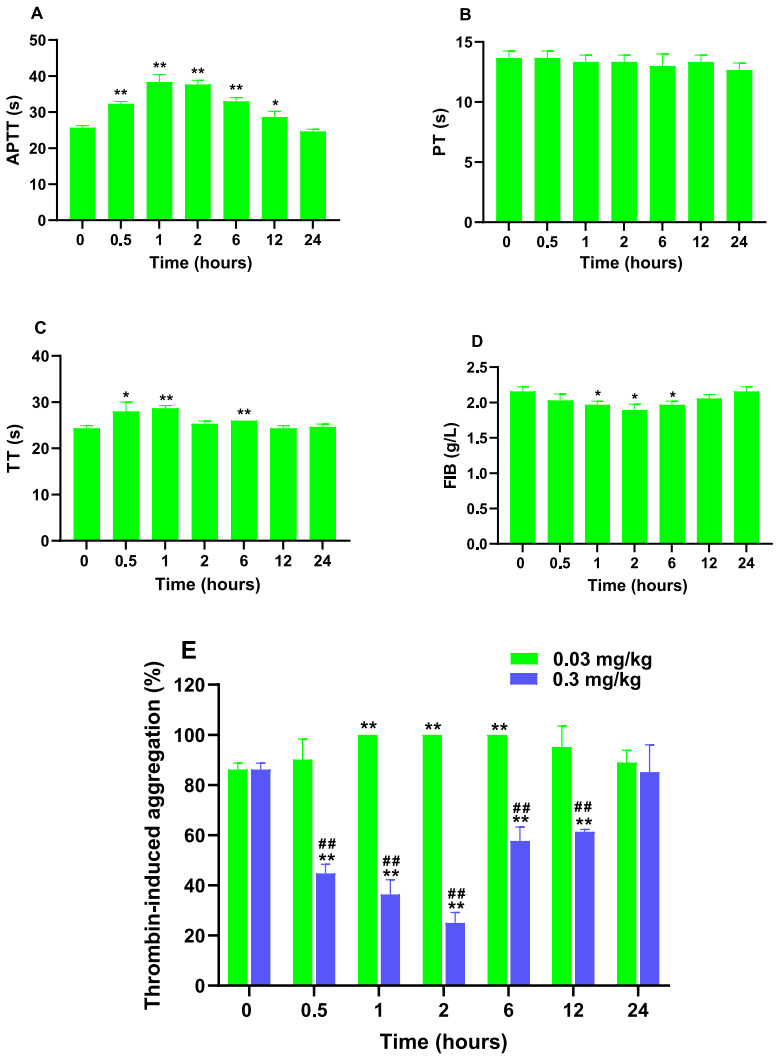

Fig. 9. Comparative assays of platelet aggregation and anticoagulation A to D represent the effects of tail vein injections of 0.03 mg/kg of atrase A in rats for 2 h, 6 h, 12 h, and 24 h on APTT, PT, TT, and FIB, respectively. E corresponds to the influence of 0.03 mg/kg and 0.3 mg/kg atrase A via tail vein injection on thrombin-induced platelet aggregation in vivo in rats at 2 h, 6 h, 12 h, and 24 h. The results are presented as the mean ± SD (n = 3). $^{*}P < 0.05$, $^{**}P < 0.01$ *vs* control. $^{\#\#}P < 0.01$ *vs* 0.03 mg/kg.

In our experiments, in addition to the significant anticoagulant activity of atrase A, a notable reduction in fibrinogen levels was observed in vivo, despite its weak fibrinogen-hydrolyzing activity in vitro. This finding suggested that atrase A induces an increase in fibrinolytic activity in vivo. To validate this hypothesis, we measured the levels of t-PA, PAI-1, and PAP in vivo after administering different doses of atrase A. Atrase A at different doses significantly increased t-PA and PAP levels at 2 h. Additionally, we examined FDP and D-dimer levels and revealed that FDP significantly increased at 1 h and 2 h, while D-dimer levels significantly increased at 2 h and 6 h, so the increase in FDP content preceded that of D-dimer. Further chromogenic substrate experiments confirmed the upregulation of plasmin activity at 0.5 h and 1 h. Moreover, the results of the chromogenic assay indicated that plasmin activity was enhanced before thrombin activity was increased. Since FDP utilizes fibrinogen as a substrate, unlike D-dimer [30]. Consequently, the reduction in fibrinogen by atrase A in vivo is attributed to the induced release of t-PA, which results in an increase in plasmin activity. Although we also observed an increase in thrombin activity and on the SDS-PAGE assay of atrase A with coagulation factor II, there were two product bands at 30–40 kDa, with molecular weights similar to those of activated thrombin light and heavy chains II [31]. However, the thrombin chromogenic assay indicated not enzyme activity was detected, and no plasma coagulation was observed during the experiments. An increase in thrombin activity may represent a protective mechanism in the body to prevent fibrin deposition [32]. Therefore, the decrease in fibrinogen content is not due to thrombin's action but rather to the combined effect of atrase A inducing the release of intrinsic t-PA. TSV-PA, a snake venom serine protease purified from the venom of *Trimeresurus stejnegeri*, is a plasminogen activator [33], another venom serine protease, batroxobin from *Bothrops atrox moojeni* venom can induce t-PA release [34]. In our

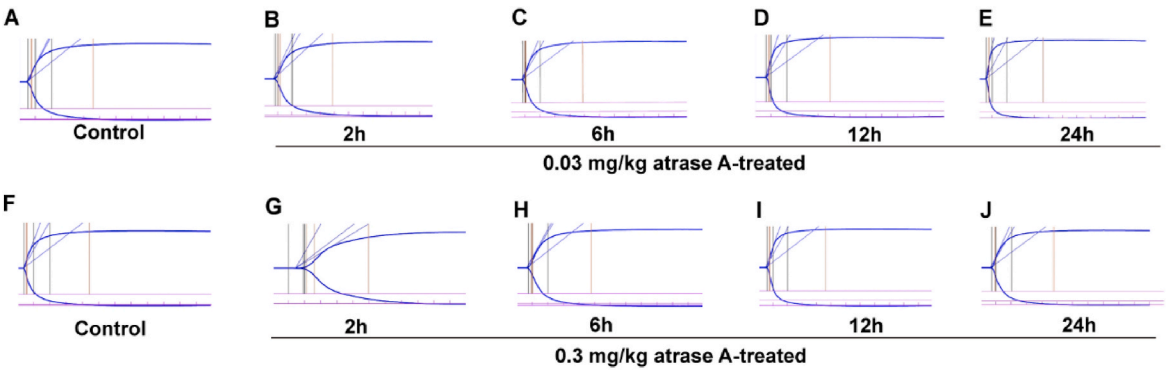

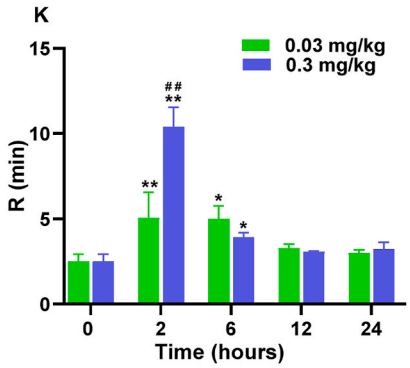

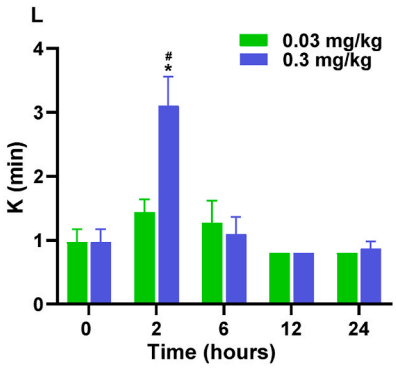

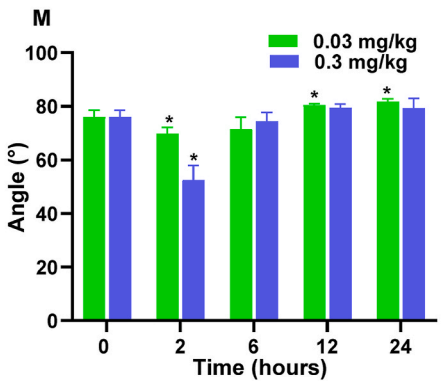

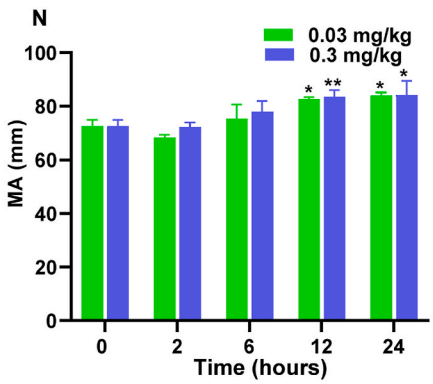

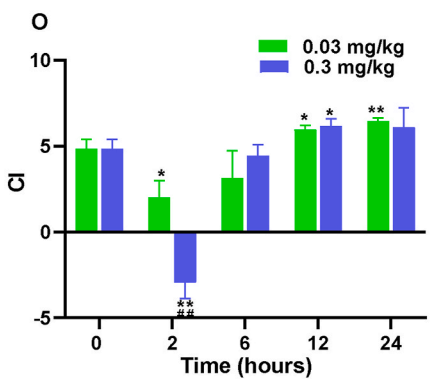

(caption on next page)

Fig. 10. The in vivo effects of atrase A were determined by thromboelastography A and F show the assay results after a 2 h tail vein injection of PBS. B to E illustrate the results at 2 h, 6 h, 12 h, and 24 h after tail vein injection of 0.03 mg/kg atrase A, respectively. G to J represent the results at 2 h, 6 h, 12 h, and 24 h after tail vein injection of 0.3 mg/kg atrase A, respectively. (K) R value represents the coagulation reaction time, with prolongation indicating coagulation factor deficiency and shortening indicating a heightened coagulation state. (L) represents the value of k. (M) represents the value of Angle. K and Angle reflect the rate of clot formation, with prolongation of K and a decrease in Angle indicating a low coagulation state and a risk of hemorrhage, while shortening of K and an increase in Angle indicate a high coagulation state and a risk of thrombosis. (N) represents the value of MA. MA represents platelet aggregation function, with a decrease in MA indicating hemorrhage and a decrease in platelet count, while an increase indicates a high coagulation state. (O) represents the value of CI. The CI is the coagulation composite index, with an increase indicating a high coagulation state and a decrease indicating a low coagulation state. The results are presented as the mean ± SD (n = 3). $^{*}P < 0.05$, $^{**}P < 0.01$ *vs* control. $^{\#}P < 0.05$, $^{\#\#}P < 0.01$ *vs* 0.03 mg/kg.

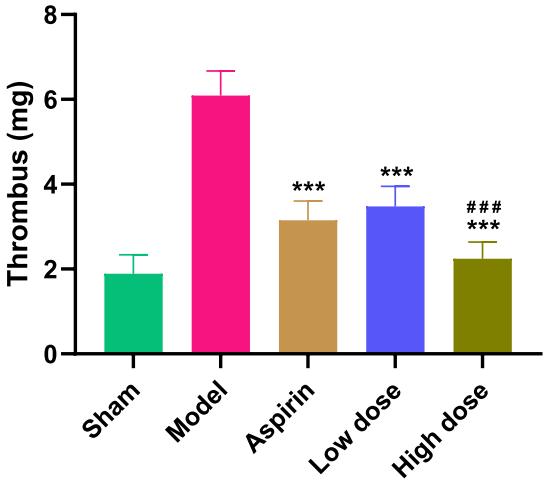

Fig. 11. Effect of atrase A on the weight of thrombi After a low dose of 0.3 mg/kg and a high dose of 3.0 mg/kg atrase A, aspirin was injected into the rats via the tail vein for 2 h, while the left common carotid artery was isolated to a length of 2 cm. In all groups except the sham-operated group, a small piece of filter paper (1 cm × 1 cm) containing 20 μL of $FeC1_3$ (2.16 mol/L) solution was applied to the left common carotid artery. In the sham-operated group, an equal amount of saline-soaked filter paper was used. After 30 min of modeling, the blood vessels at the site of thrombosis in the left common carotid artery were promptly excised, placed on filter paper to absorb any residual blood, and weighed using an electronic analytical balance. The results are presented as the mean ± SD (n = 8–9). $^{***}P < 0.001$ *vs* model. $^{\#\#\#}P < 0.001$ *vs* aspirin.

knowledge, no SVMP has been reported to possess the ability to induce the release of t-PA. However, the mechanisms underlying the induction of endogenous t-PA release by atrase A require further investigation.

From the aforementioned experiments, we deduce that atrase A achieves its effects through the combination of coagulation factor VIII inhibition, fibrinogen reduction, and platelet aggregation inhibition. These effects became evident at a dose of 0.3 mg/kg. To determine which of these effects play a pivotal role in anticoagulation, we reduced the in vivo dose of atrase A to 0.03 mg/kg. Even at this lower dose, APTT remained significantly prolonged, thromboelastography showed hypocoagulability, and there was no significant change in platelet function. The anticoagulant activity of atrase A was still apparent when 0.03 mg/kg was compared with 0.3 mg/kg. However, it had no significant effect on reducing fibrinogen levels and did not inhibit thrombin-induced platelet aggregation. This finding suggested that atrase A primarily exerts its anticoagulant effect by initially inhibiting coagulation factors, followed by a reduction in fibrinogen levels and ultimately inhibition of platelet aggregation.

The experimental findings demonstrate the potent anticoagulant activity of atrase A, piquing our interest in exploring its potential to prevent thrombosis. To investigate this possibility, we tested whether atrase A could prevent $FeCl_3$-induced carotid artery thrombosis in rats using an animal thrombosis model. The results revealed that atrase A significantly inhibited thrombus formation at doses of 0.3 mg/kg and 3 mg/kg, with an effect comparable to that of the positive control drug at a lower dose. This experiment underscores the substantial inhibitory effect of atrase A on thrombus formation.

The current study revealed that SVMPs exhibit different activities such as hydrolyzing of fibrinogen or fibrin, action of thrombin or inhibition of platelet aggregation [35]. For example, the P–I class BnP1 from *B. neuwiedi* venom and the P-III class Jararhagin from *Bothrops jararaca* venom directly hydrolyze fibrinogen and fibrin [36–38], HF3 and bothropasin from *Bothrops jararaca* inhibit platelet aggregation [39], Mocarhagin isolated from *Naja* venom inhibits platelet aggregation by cleaving GPIb [15], Berythractivase from *Bothrops erythromelas*, which acts as a thrombinogen activator [40].

To the best of our knowledge, no SVMPs have been reported to target intrinsic or extrinsic pathway coagulation factors. Atrase A, the first elapid venom P-III class metalloproteinase demonstrated to cleave coagulation factor VIII, also reduces in vivo fibrinogen

levels through a novel mechanism involving the release of t-PA. This mechanism sets atrase A apart from other SVMPs. Studies have highlighted the importance of the intrinsic pathway in venous thrombosis, with elevated levels of coagulation factor VIII associated with a greater risk of venous thrombosis [41,42]. t-PA, which reduces fibrinogen levels, is a crucial component of current thrombolytic therapy and plays a pivotal role in thrombolysis [43].

6. Conclusion

The mechanism of action of atrase A involves impacting the intrinsic pathway by cleaving coagulation factor VIII and inducing the release of endogenous t-PA. As a novel anticoagulant strategy, the mechanism of action of atrase A aligns with the development of new drugs that could support thrombolytic therapy. Atrase A has emerged as a promising candidate for the development of novel anticoagulant drugs.

Data availability

Data will be available upon request.

CRediT authorship contribution statement

Xin-Jie Zhong: Writing – original draft, Formal analysis, Data curation. **Cai-E Wang:** Data curation. **Ya-Nan Li:** Data curation. **Qi-Yun Zhang:** Data curation. **Qian-Yun Sun:** Writing – review & editing, Supervision, Methodology, Investigation, Funding acquisition, Data curation, Conceptualization.

Declaration of competing interest

The authors declare that they have no known competing financial interests or personal relationships that could have appeared to influence the work reported in this paper.

Acknowledgments

This work was supported by funding from National Natural Science Foundation of China (No. 32160129 and 81260494) and Guizhou Provincial Science and Technology Projects (QKHZC 2018–2828).

Appendix A. Supplementary data

Supplementary data to this article can be found online at https://doi.org/10.1016/j.heliyon.2024.e30969.

Abbreviations

APTT	Activated partial thromboplastin time
TT	Thrombin time;
PT	Prothrombin time
FIB	Fibrinogen
SVMPs	Snake venom metalloproteinases
AA	Arachidonic acid
ADP	Adenosin diphosphate
Thr	Thrombin
FDP	Fibrinogen degradation product
t-PA	Tissue-type fibrinogen activator
PAP	Fibrinase-*anti*-fibrinolytic enzyme complex
PAI-1	Fibrinogen activation inhibitor-1
PMV	Protobothrops mucrosquamatus
PRP	platelet-rich plasma
PPP	platelet-poor plasma
PVDF	Polyvinylidene fluoride
SDS-PAGE	Sodium dodecyl sulfate-polyacrylamide gel electrophoresis
S2238	Chromogenic substrate for Thrombin
S2251	Chromogenic substrate for plasmin and streptokinase-activated plasminogen
ELISA	Enzyme-linked immunosorbent assay

References

[1] C. Knudsen, J.A. Jürgensen, S. Føns, A.M. Haack, R.U.W. Friis, S.H. Dam, S.P. Bush, J. White, A.H. Laustsen, Snakebite envenoming diagnosis and Diagnostics, Front. Immunol. 12 (2021) 661457, https://doi.org/10.3389/fimmu.2021.661457.

[2] J.M. Gutiérrez, J.J. Calvete, A.G. Habib, R.A. Harrison, D.J. Williams, D.A. Warrell, Snakebite envenoming, Nat. Rev. Dis. Prim. 3 (2017) 17063, https://doi.org/10.1038/nrdp.2017.63.

[3] N.R. Casewell, T.N.W. Jackson, A.H. Laustsen, K. Sunagar, Causes and consequences of snake venom variation, Trends Pharmacol. Sci. 41 (2020) 570–581, https://doi.org/10.1016/j.tips.2020.05.006.

[4] A. Munawar, S. Ali, A. Akrem, C. Betzel, Snake venom peptides: tools of biodiscovery, Toxins 10 (2018) 474, https://doi.org/10.3390/toxins10110474.

[5] T. Tasoulis, G. Isbister, A review and database of snake venom proteomes, Toxins 9 (2017) 290, https://doi.org/10.3390/toxins9090290.

[6] C.-C. Liu, C.-C. Lin, Y.-C. Hsiao, P.-J. Wang, J.-S. Yu, Proteomic characterization of six Taiwanese snake venoms: identification of species-specific proteins and development of a SISCAPA-MRM assay for cobra venom factors, J. Proteonomics 187 (2018) 59–68, https://doi.org/10.1016/j.jprot.2018.06.003.

[7] A.L. Oliveira, M.F. Viegas, S.L. Da Silva, A.M. Soares, M.J. Ramos, P.A. Fernandes, The chemistry of snake venom and its medicinal potential, Nat. Rev. Chem 6 (2022) 451–469, https://doi.org/10.1038/s41570-022-00393-7.

[8] S. Takeda, H. Takeya, S. Iwanaga, Snake venom metalloproteinases: structure, function and relevance to the mammalian ADAM/ADAMTS family proteins, Biochim. Biophys. Acta Protein Proteonomics 1824 (2012) 164–176, https://doi.org/10.1016/j.bbapap.2011.04.009.

[9] E. Sanchez, R. Flores-Ortiz, V. Alvarenga, J. Eble, Direct fibrinolytic snake venom metalloproteinases affecting hemostasis: structural, biochemical features and therapeutic potential, Toxins 9 (2017) 392, https://doi.org/10.3390/toxins9120392.

[10] J. Gutiérrez, T. Escalante, A. Rucavado, C. Herrera, Hemorrhage caused by snake venom metalloproteinases: a journey of discovery and understanding, Toxins 8 (2016) 93, https://doi.org/10.3390/toxins8040093.

[11] J.W. Fox, S.M.T. Serrano, Structural considerations of the snake venom metalloproteinases, key members of the M12 reprolysin family of metalloproteinases, Toxicon 45 (2005) 969–985, https://doi.org/10.1016/j.toxicon.2005.02.012.

[12] J.W. Fox, S.M.T. Serrano, Insights into and speculations about snake venom metalloproteinase (SVMP) synthesis, folding and disulfide bond formation and their contribution to venom complexity: snake venom metalloproteinases and venom complexity, FEBS J. 275 (2008) 3016–3030, https://doi.org/10.1111/j.1742-4658.2008.06466.x.

[13] J.J. Calvete, Venomics: integrative venom proteomics and beyond, Biochem. J. 474 (2017) 611–634, https://doi.org/10.1042/BCJ20160577.

[14] J. Gutiérrez, T. Escalante, A. Rucavado, C. Herrera, J. Fox, A comprehensive view of the structural and functional alterations of extracellular matrix by snake venom metalloproteinases (SVMPs): novel perspectives on the pathophysiology of envenoming, Toxins 8 (2016) 304, https://doi.org/10.3390/toxins8100304.

[15] C.M. Ward, D.V. Vinogradov, R.K. Andrews, M.C. Berndt, Characterization of mocarhagin, a cobra venom metalloproteinase from Naja mocambique mocambique, and related proteins from other Elapidae venoms, Toxicon 34 (1996) 1203–1206, https://doi.org/10.1016/0041-0101(96)00115-8.

[16] O.T. Olaoba, P. Karina Dos Santos, H.S. Selistre-de-Araujo, D.H. Ferreira De Souza, Snake venom metalloproteinases (SVMPs): a structure-function update, Toxicon X 7 (2020) 100052, https://doi.org/10.1016/j.toxcx.2020.100052.

[17] A.F. Asega, M.C. Menezes, D. Trevisan-Silva, D. Cajado-Carvalho, L. Bertholim, A.K. Oliveira, A. Zelanis, S.M.T. Serrano, Cleavage of proteoglycans, plasma proteins and the platelet-derived growth factor receptor in the hemorrhagic process induced by snake venom metalloproteinases, Sci. Rep. 10 (2020) 12912, https://doi.org/10.1038/s41598-020-69396-y.

[18] J. Wei, Y. Mo, L. Qiao, X. Wei, H. Chen, H. Xie, Y. Fu, W. Wang, Y. Xiong, S. He, Potent histamine-releasing activity of atrahagin, a novel snake venom metalloproteinase, Int. J. Biochem. Cell Biol. 38 (2006) 510–520, https://doi.org/10.1016/j.biocel.2005.10.011.

[19] C. Baldo, C. Jamora, N. Yamanouye, T.M. Zorn, A.M. Moura-da-Silva, Mechanisms of vascular damage by hemorrhagic snake venom metalloproteinases: tissue distribution and in situ hydrolysis, PLoS Neglected Trop. Dis. 4 (2010) e727, https://doi.org/10.1371/journal.pntd.0000727.

[20] T. Escalante, A. Rucavado, J.W. Fox, J.M. Gutiérrez, Key events in microvascular damage induced by snake venom hemorrhagic metalloproteinases, J. Proteonomics 74 (2011) 1781–1794, https://doi.org/10.1016/j.jprot.2011.03.026.

[21] C. Herrera, T. Escalante, M.-B. Voisin, A. Rucavado, D. Morazán, J.K.A. Macêdo, J.J. Calvete, L. Sanz, S. Nourshargh, J.M. Gutiérrez, J.W. Fox, Tissue localization and extracellular matrix degradation by PI, PII and PIII snake venom metalloproteinases: clues on the mechanisms of venom-induced hemorrhage, PLoS Neglected Trop. Dis. 9 (2015) e0003731, https://doi.org/10.1371/journal.pntd.0003731.

[22] R. Kini, C. Koh, Metalloproteases affecting blood coagulation, fibrinolysis and platelet aggregation from snake venoms: definition and nomenclature of interaction sites, Toxins 8 (2016) 284, https://doi.org/10.3390/toxins8100284.

[23] A.M. Moura-da-Silva, O.H.P. Ramos, C. Baldo, S. Niland, U. Hansen, J.S. Ventura, S. Furlan, D. Butera, M.S. Della-Casa, I. Tanjoni, P.B. Clissa, I. Fernandes, A. M. Chudzinski-Tavassi, J.A. Eble, Collagen binding is a key factor for the hemorrhagic activity of snake venom metalloproteinases, Biochimie 90 (2008) 484–492, https://doi.org/10.1016/j.biochi.2007.11.009.

[24] Q.Y. Sun, M. Li, M.F. Yang, Purification and characterization of a metalloproteinase with weak fibrinogenolytic activity from Naja atra venom, Chinese Journal of Biochemistry and Molecular Biology 23 (2007) 835–843, https://doi.org/10.3969/j.issn.1007-7626.2007.10.008.

[25] Q.Y. Sun, J. Bao, Purification, cloning and characterization of a metalloproteinase from Naja atra venom, Toxicon 56 (2010) 1459–1469, https://doi.org/10.1016/j.toxicon.2010.08.013.

[26] S. Butenas, K.G. Mann, Blood coagulation, Biochemistry. Biokhimiia 67 (2002) 3–12, https://doi.org/10.1023/a:1013985911759.

[27] C.E. Wang, Q.Y. Sun, M. Li, J.S. Shi, Antiplatelet aggregation effect and mechanism of cobra venom metalloproteinase atrase A, Chinese Journal of Pharmacological Bulletin 25 (2009) 743–747.

[28] R.M. Camire, Blood coagulation factor X: molecular biology, inherited disease, and engineered therapeutics, J. Thromb. Thrombolysis 52 (2021) 383–390, https://doi.org/10.1007/s11239-021-02456-w.

[29] P.J. Fay, Activation of factor VIII and mechanisms of cofactor action, Blood Rev. 18 (2004) 1–15, https://doi.org/10.1016/S0268-960X(03)00025-0.

[30] J.I. Weitz, J.C. Fredenburgh, J.W. Eikelboom, A test in context: D-dimer, J. Am. Coll. Cardiol. 70 (2017) 2411–2420, https://doi.org/10.1016/j.jacc.2017.09.024.

[31] W.E. Winter, D.N. Greene, S.G. Beal, J.A. Isom, H. Manning, G. Wilkerson, N. Harris, Clotting factors: clinical biochemistry and their roles as plasma enzymes, in: Advances in Clinical Chemistry, Elsevier, 2020, pp. 31–84, https://doi.org/10.1016/bs.acc.2019.07.008.

[32] P. Gaffney, Breakdown products of fibrin and fibrinogen: molecular mechanisms and clinical implications, J. Clin. Pathol. Suppl., 14, 10–17.

[33] Y. Zhang, A. Wisner, Y. Xiong, C. Bon, A novel plasminogen activator from snake venom, J. Biol. Chem. 270 (1995) 10246–10255, https://doi.org/10.1074/jbc.270.17.10246.

[34] D. Lan, S. Song, Y. Liu, B. Jiao, R. Meng, Use of batroxobin in central and peripheral ischemic vascular diseases: a systematic review, Front. Neurol. 12 (2021) 716778, https://doi.org/10.3389/fneur.2021.716778.

[35] E. Oyama, H. Takahashi, Structures and functions of snake venom metalloproteinases (SVMP) from Protobothrops venom collected in Japan, Molecules 22 (2017) 1305, https://doi.org/10.3390/molecules22081305.

[36] C. Baldo, I. Tanjoni, I.R. León, I.F.C. Batista, M.S. Della-Casa, P.B. Clissa, R. Weinlich, M. Lopes-Ferreira, I. Lebrun, G.P. Amarante-Mendes, V.M. Rodrigues, J. Perales, R.H. Valente, A.M. Moura-da-Silva, BnP1, a novel P-I metalloproteinase from Bothrops neuwiedi venom: biological effects benchmarking relatively to jararhagin, a P-III SVMP, Toxicon 51 (2008) 54–65, https://doi.org/10.1016/j.toxicon.2007.08.005.

[37] A.M. Moura-da-Silva, C. Baldo, Jararhagin, a hemorrhagic snake venom metalloproteinase from Bothrops jararaca, Toxicon 60 (2012) 280–289, https://doi.org/10.1016/j.toxicon.2012.03.026.

[38] M. Sugiki, M. Maruyama, E. Yoshida, H. Mihara, A.S. Kamiguti, R.DavidG. Theakston, Enhancement of plasma fibrinolysis in vitro by jararhagin, the main haemorrhagic metalloproteinase in Bothrops jararaca venom, Toxicon 33 (1995) 1605–1617, https://doi.org/10.1016/0041-0101(95)00102-6.

[39] A.K. Oliveira, A.F. Paes Leme, M.T. Assakura, M.C. Menezes, A. Zelanis, A.K. Tashima, M. Lopes-Ferreira, C. Lima, A.C.M. Camargo, J.W. Fox, S.M.T. Serrano, Simplified procedures for the isolation of HF3, bothropasin, disintegrin-like/cysteine-rich protein and a novel P-I metalloproteinase from Bothrops jararaca venom, Toxicon 53 (2009) 797–801, https://doi.org/10.1016/j.toxicon.2009.02.019.

[40] M.B. Silva, M. Schattner, C.R.R. Ramos, I.L.M. Junqueira-de-Azevedo, M.C. Guarnieri, M.A. Lazzari, C.A.M. Sampaio, R.G. Pozner, J.S. Ventura, P.L. Ho, A. M. Chudzinski-Tavassi, A prothrombin activator from Bothrops erythromelas (jararaca-da-seca) snake venom: characterization and molecular cloning, Biochem. J. 369 (2003) 129–139, https://doi.org/10.1042/bj20020449.

[41] I.M. Rietveld, W.M. Lijfering, S. Le Cessie, M.H.A. Bos, F.R. Rosendaal, P.H. Reitsma, S.C. Cannegieter, High levels of coagulation factors and venous thrombosis risk: strongest association for factor VIII and von Willebrand factor, J. Thromb. Haemostasis 17 (2019) 99–109, https://doi.org/10.1111/jth.14343.

[42] T. Bombeli, M. Jutzi, E. De Conno, B. Seifert, J. Fehr, In patients with deep-vein thrombosis elevated levels of factor VIII correlate only with von Willebrand factor but not other endothelial cell-derived coagulation and fibrinolysis proteins, Blood Coagul. Fibrinolysis 13 (2002) 577–581, https://doi.org/10.1097/00001721-200210000-00001.

[43] G. Agnelli, Rationale for bolus t-PA therapy to improve efficacy and safety, Chest 97 (1990) 161S–167S, https://doi.org/10.1378/chest.97.4_Supplement.161S.